Available online at www.sciencedirect.com
ScienceDirect
Mendeleev Commun., 2012, **22**, 159–161
Mendeleev Communications

A comparative study of immunoglobulin IgM and rheumatoid factor IgMRF in solution by small-angle X-ray scattering

Vladimir V. Volkov,*[a] Victor A. Lapuk,[b] Anna I. Toropova,[c] Elena Yu. Varlamova,[d] Eleonora V. Shtykova,[a] Kirill A. Dembo[a] and Vladimir P. Timofeev[e]

[a] *A. V. Shubnikov Institute of Crystallography, Russian Academy of Sciences, 119333 Moscow, Russian Federation. E-mail: vvo@ns.crys.ras.ru*
[b] *N. D. Zelinsky Institute of Organic Chemistry, Russian Academy of Sciences, 119991 Moscow, Russian Federation*
[c] *D. V. Skobeltsyn Institute of Nuclear Physics, M. V. Lomonosov Moscow State University, 119991 Moscow, Russian Federation*
[d] *Hematology Research Center, Russian Academy of Medical Sciences, 125167 Moscow, Russian Federation*
[e] *M. M. Shemyakin–Yu. A. Ovchinnikov Institute of Bioorganic Chemistry, Russian Academy of Sciences, 117997 Moscow, Russian Federation*

DOI: 10.1016/j.mencom.2012.05.017

The shapes of rheumatoid factor molecules calculated from X-ray small-angle solution scattering data suggest that the peripheral Fab regions of rheumatoid factor in solution are more flocculent because of a higher flexibility of Fab domains.

Rheumatoid immunoglobulin M (IgMRF) belongs to a group of rheumatoid factors (RFs), which are autoantibodies against proteins of the own organism. It is widely known that IgMRF, like other RFs, plays an important role in the pathogenesis of rheumatoid arthritis[1] and autoimmune diseases such as systemic lupus erythematosus and Sjögren's syndrome, as well as in chronic infectious diseases. Therefore, it is of interest to study the structure–function relationships for RFs. This work is focused on IgMRF, which dominates among RFs. The macromolecules of both non-rheumatoid immunoglobulin M (IgM) and IgMRF consist of five IgG-like monomers. The latter compounds are crystallizable, and their structures were determined by X-ray crystallographic methods[2–4] providig a possibility to build structural models of both IgM and IgMRF, which could not be crystallized. Earlier studies[5–8] suggest that differences between IgM and IgMRF should be in the Fab regions because they contain the antigen-binding sites responsible for the antibody function. Structural differences between the Fab regions of IgM and IgMRF found[8] from SAXS data pointed to a higher asymmetry of Fab-RF pairs and a lower molecular mass of the entire IgMRF. The conclusion[9] that the Fab fragments of IgMRF are much more flexible than Fab in IgM and, at the same time, have the same globular shape was also used here for molecular modeling.

The samples of human monoclonal IgM and rheumatoid factor IgMRF (Waldenström's disease) were prepared according to published procedures[10,11] with concentrations from 2.3 to 12.5 mg ml^{-1} (samples IgM1–IgM3 and IgMRF1–IgMRF3, respectively). The RF sample with an enormous rheumatoid activity of 32 600 IU ml^{-1} at a normal rate of 0–20 (in the following, IgMRF$\varkappa$) was obtained at a concentration of 12.5 mg ml^{-1} using the same procedures from the blood plasma of another patient. This sample contained <3.7% IgG in the complex IgMRF$\varkappa$-IgG and trace amounts of α2-macroglobulin. A Tris buffer (Merck) was used as a solvent at pH 8.3–8.4.

An AMUR-K laboratory small-angle X-ray diffractometer (Institute of Crystallography) was used to measure IgM3, IgMRF3 and IgMRF$\varkappa$ at the wavelength $\lambda = 0.1542$ nm (CuKα) with Kratky beam geometry 0.2×8.0 mm and 3300-channel linear position-sensitive detector OD3. The angular range was $0.1 < s < 12.0$ nm^{-1}, where s is the modulus of the scattering vector $s = 4\pi \sin(\theta/\lambda)$, 2θ is the scattering angle. 1.0 mm quartz capillaries for X-ray measurements were used elsewhere. Synchrotron data[9] for IgM1–IgM3, IgMRF1, and IgMRF2 were used. All the experimental data were normalized to the incident beam intensity (the measurements were followed by correction for the collimation effects according to a standard procedure[12]). Finally, the buffer scattering was subtracted from the solution data.

Distance distribution functions $p(r)$ were calculated from the well-known relation using the regularized indirect Fourier transform program GNOM:[13]

$$p(r) = \frac{1}{2\pi^2} \int_{s=0}^{\infty} I(s) \frac{\sin(sr)}{sr} \mathrm{d}s,$$

where the scattering intensity $I(s)$ was given in arbitrary units. The regularization parameter 'alpha', which is used to smooth and stabilize the solution, was manually adjusted by reducing 3–10 times to clarify the difference between $p(r)$ calculated for IgM, IgMRF, and IgMRF$\varkappa$ at large distances r. Checking for possible aggregation of molecules was performed by a comparison of gyration radii R_g calculated from the initial part of $I(s)$ using the Guinier relation $I_{exp}(s) \approx I(0)(1 - s^2R_g^2/3)$ at $sR_g < 1.5$, and from the integral

$$I_{exp}(s) \approx I(0)\left[1 - \frac{s^2}{3}\left(\int_0^D r^2 p(r)\mathrm{d}r \Big/ 2\int_0^D p(r)\mathrm{d}r\right)\right].$$

The latter estimate is much less influenced by aggregation effects. The shapes of calculated $p(r)$ functions were also used to determine the maximum sizes D_{max} of dissolved molecules.

The shapes of macromolecules were found using the modified DAMMIN[14] and GASBOR[15] programs. Both of the algorithms are based on modeling the particle structure by small elements (spheres in DAMMIN and amino acid residues in GASBOR) and the least-squares fitting of experimental scattering intensity by a global minimization method based on simulated annealing random search of spatial arrangement of elements. Amino acid sequences for IgM and its components were taken from the atomic structure 2RCJ built by Perkins *et al.*[16] using small-angle X-ray scattering (SAXS) data obtained from IgM solutions and crystal structures of crystallizable fragments.

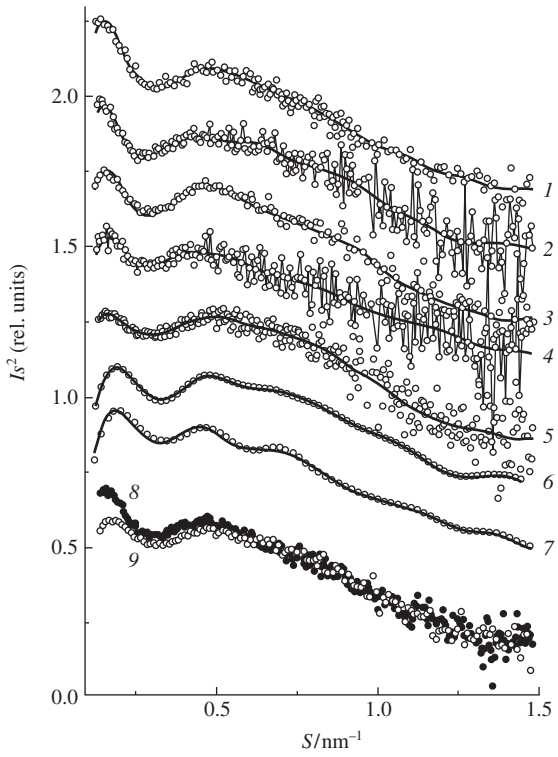

Figure 1 SAXS patterns (dots) and scattering from models (smooth solid lines) for protein solutions (Kratky plot). (*1*) IgM1, (*2*) IgM2, (*3*) IgM3, (*4*) IgMRF1, (*5*) IgMRF2, (*6*) IgMRF3, (*7*) IgMRF$\varkappa$, (*8*) averaged scattering patterns for all IgM samples, (*9*) averaged SAXS intensities for all RF samples (open circles). All curves are shifted vertically for better visualization. Curves *8* and *9* are matched in the region $0.5 < s < 1.0$ nm^{-1} to clarify their difference at $s < 0.5$ nm^{-1}, which is rather small but systematic.

The scattering patterns from protein solutions are shown in Figure 1. The distance distribution functions calculated from SAXS data show a systematic difference (Figure 2) in spite of the apparent similarity of scattering patterns (Figure 1, curves *8* and *9*), in the range $s > 0.5$ nm^{-1}. Pairwise matched data IgM–IgMRF demonstrate slight difference in scattering shapes: IgMRF data go systematically lower at the beginning ($s < 0.5$ nm^{-1}) (Figure 1, curves *8* and *9*), which points to smaller molecular dimensions of RF molecules. The systematic leftwise displacement of $p(r)$ profiles for RFs points to the shift of molecular density to the center for all RF particles. The same conclusion can be made from dimension parameters presented in Table 1. The differences might be described by structures in which some Fab fragments are shifted to the centre of the molecule.

Molecular shapes calculated *ab initio* (only a 5th order symmetry axis was introduced in the models during the search) using DAMMIN confirm conclusions about less size of RF and its

Table 1 Dimension parameters of *ab initio* structural models calculated by DAMMIN. The values were obtained by averaging from 10 to 50 independently obtained structures for each scattering pattern.

Sample	R_g (Guinier)/ nm	R_g from $p(r)$/nm	D_{max}/nm	Excluded volume for model/nm^3
IgM1	124±2	124±3	390±10	1300±100
IgM2	127±2	126±3	395±5	1200±130
IgM3	128±2	129±2	410±10	1390±100
Average values	126±3	126±3	398±15	1300±150
IgMRF1	111±2	111±7	360±10	1200±110
IgMRF2	116±2	116±1	380±5	1350±100
IgMRF3	108±2	108±4	370±10	1000±80
Average values	113±4	113±6	370±15	1200±250
IgMRF$\varkappa$	106±2	106±3	370±20	780±80

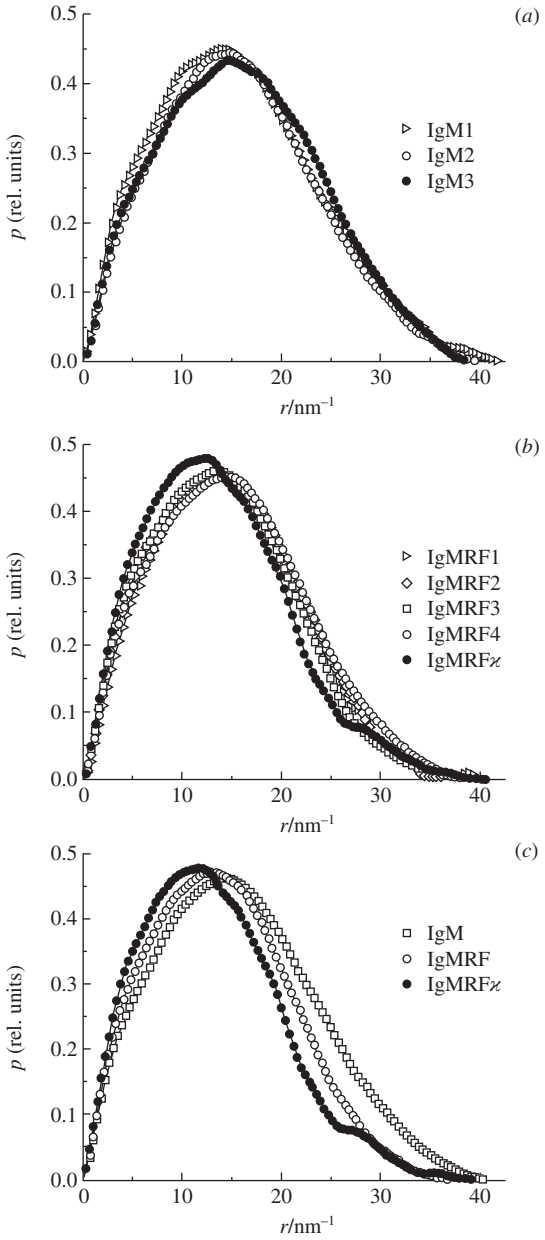

Figure 2 Comparison of distance distribution functions $p(r)$ calculated from SAXS data. Groups *a* and *b* show distinct distributions for each sample, group *c* demonstrates difference between averaged distributions.

peripheral structural flocculency for all samples of RFs. χ^2 values for the fits were in the range of 0.8–1.1, *i.e.* within the limits of random measurement errors. Some of the typical models are shown in Figure 3(*b*)–(*f*). Attention is drawn to the fact that for IgMRF$\varkappa$ sample the averaged model volume is significantly less than for IgMRF samples, as it can be seen in Table 1. The distance distribution function of IgMRF$\varkappa$ is also shifted to the left much more and this led to the atomic model shown in Figure 3(*d*). It is characterized by each second Fab in the pair being reduced by detaching light chain and simultaneously rotated to the centre of the molecule. To obtain this result, a series of molecular models was manually built from the molecular fragments of 2RCJ using the MASSHA program.[17] Theoretical scattering from these atomic structures was calculated by the CRYSOL program[18] and χ^2 values were in the range of 2.5–4.1 due to oscillations in the middle part of the model SAXS patterns because of the high symmetry of the central Fc5 fragment, which was considered a constant part. Checking of IgMRF$\varkappa$ models, which contain a reduced number of Fab's (1–9 instead of normally 10) placed in different positions, rotated by different angles, and taken with different combinations

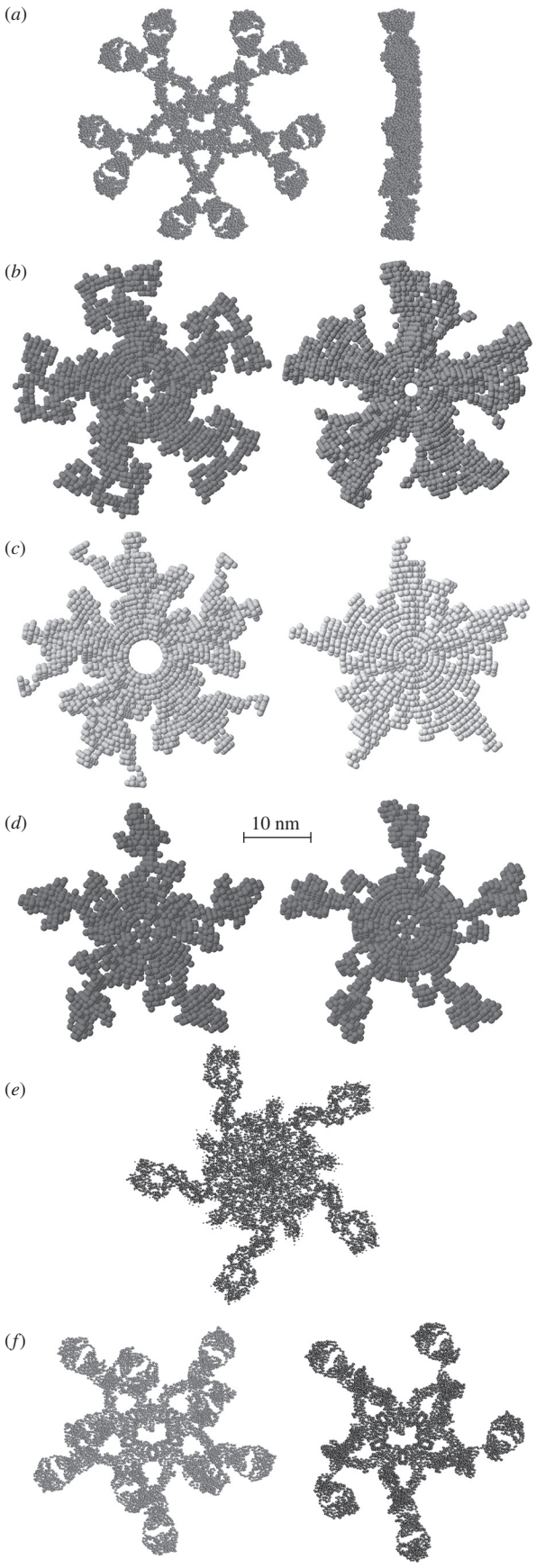

Figure 3 Structure models: (*a*) IgM (2RCJ[16] shown in two orientations); (*b*) two typical models of IgM by DAMMIN; (*c*) two typical models of IgMRF by DAMMIN; (*d*) two typical models of IgMRFκ by DAMMIN; (*e*) model IgMRFκ by GASBOR; (*f*) manually constructed models of IgMRF (left) and IgMRFκ (right) which show the best fit to the experimental data. Typical fits to the experimental scattering patterns are shown in Figure 1 by smooth solid lines.

showed that the χ^2 values are systematically larger (by a factor of 1.3–5) than those for models built from both normal and reduced Fab's. Another reason for building this 'flocculent' model of IgMRFκ was a pair of typical *ab initio* shapes obtained by DAMMIN and GASBOR [Figure 3(*d*),(*e*)]. As to IgM and IgMRF atomic models it was necessary only rotate Fab fragments without reducing their number and structure [Figure 3(*f*)]. Violations of the spatial ordering of Fab fragments in 2RCJ model flatten SAXS curves and correspond to the expected flexibility of IgM. A comparison of obtained structures with published models[19] shows that a more flat conformation of both IgM and IgMRF is observed in the solution.

SAXS experiments for the extended set of samples have confirmed that the major difference between intact immunoglobulin M and two rheumatoid factors separated from two blood plasma samples is in the depleted peripheral regions occupied by Fab fragments due to their increased flexibility and mobility.

We are grateful to the staff of the European Molecular Biology Laboratory for their participation in measurements and discussions and especially to the head of the SAXS Group D. Svergun for a valuable contribution.

References

1 B. Sutton, A. Corper, V. Bonagura and M. Taussig, *Immunol. Today*, 2000, **21**, 177.
2 L. J. Harris, S. B. Larson, K. W. Hasel, J. Day, A. Greenwod and A. McPherson, *Nature*, 1992, **360**, 369.
3 L. J. Harris, E. Skaletsky and A. McPherson, *J. Mol. Biol*., 1998, **275**, 861.
4 L. J. Harris, S. B. Larson and A. McPherson, *Adv. Immunol*., 1998, **72**, 191.
5 V. A. Lapuk, V. Ya. Chernyak and N. N. Magretova, *Biokhimiya*, 1996, **61**, 85 [*Biochemistry (Moscow)*, 1996, **61**, 61].
6 I. I. Protasevich, V. Ranzhbar, E. Yu. Varlamova, A. Cherkasov and V. A. Lapuk, *Biokhimiya*, 1997, **62**, 1066 (in Russian).
7 V. V. Volkov, R. L. Kayushina, V. A. Lapuk, E. V. Shtykova, E. Yu. Varlamova, M. Malfois and D. I. Svergun, *Kristallografiya*, 2003, **48**, 103 (*Crystallography Reports*, 2003, **48**, 98).
8 V. V. Volkov, V. A. Lapuk, R. L. Kayushina, E. V. Shtykova, E. Yu. Varlamova, M. Malfoisde and D. I. Svergun, *J. Appl. Crystallogr*., 2003, **36**, 503.
9 V. V. Volkov, V. A. Lapuk, E. V. Shtykova, N. D. Stepina, K. A. Dembo, A. V. Sokolova, S. V. Amarantov, V. P. Timofeev, R. Kh. Ziganshin and E. Yu. Varlamova, *Kristallografiya*, 2008, **53**, 499 (*Crystallography Reports*, 2008, **53**, 466).
10 V. A. Lapuk, N. M. Khatiashvili, A. I. Chukhrova and E. D. Kaverzneva, *Biokhimiya*, 1985, **50**, 237 (in Russian).
11 V. A. Lapuk, A. I. Chukhrova, E. V. Chernokhvostova, V. A. Aleshkin, G. P. German, E. Yu. Varlamova, A. M. Ponomareva, N. P. Arbatskii and A. O. Zheltova, *Biokhimiya*, 1992, **57**, 617 (in Russian).
12 L. A. Feigin and D. I. Svergun, *Structure Analysis by Small-Angle X-ray and Neutron Scattering*, Plenum Press, New York, 1987, p. 363.
13 D. I. Svergun, *J. Appl. Crystallogr*., 1992, **25**, 495.
14 D. I. Svergun, *Biophys. J.*, 1999, **76**, 2879.
15 D. I. Svergun, M. V. Petoukhov and M. H. J. Koch, *Biophys. J*., 2001, **80**, 2946.
16 S. J. Perkins, A. S. Nealis, B. J. Sutton and A. Feinstein, *J. Mol. Biol*., 1991, **21**, 1345.
17 P. V. Konarev, M. V. Petoukhov and D. I. Svergun., *J. Appl. Crystallogr*., 2001, **34**, 527.
18 D. Svergun, C. Barberato and M. H. J. Koch, *J. Appl. Crystallogr*., 1995, **28**, 768.
19 D. M. Czajkowsky and Z. Shao, *Proc. Natl. Acad. Sci. USA*, 2009, **106**, 14960.

Received: 10th November 2011; Com. 11/3835